# Drift Reversal Capability in Helical Systems

M.Yokoyama 1), K.Itoh 1), S.Okamura 1), K.Matsuoka 1), N.Nakajima 1), S.-I.Itoh 2), G. H. Neilson 3), M. C. Zarnstorff 3) and G.Rewoldt 3)

1) National Institute for Fusion Science, 322-6 Oroshi, Toki 509-5292, Japan
2) Research Institute for Applied Mechanics, Kyushu University, Kasuga 816-8580, Japan
3) Princeton Plasma Physics Laboratory, Princeton, NJ 08543, USA

e-mail contact of main author: yokoyama@nifs.ac.jp

**Abstract.** The maximum-$J$ ($J$ is the second adiabatic invariant) capability, i.e., the drift reversal capability, is examined in quasi-axisymmetric (QAS) stellarators and quasi-poloidally symmetric (QPS) stellarators as a possible mechanism for turbulent transport suppression. Due to the existence of non-axisymmetry of the magnetic field strength in QAS configurations, a local maximum of $J$ is created to cause the drift reversal. The increase of magnetic shear in finite beta equilibria also has favorable effect in realizing the drift reversal. The radial variation of the uniform magnetic field component plays a crucial role for the drift reversal in a QPS configuration. Thus, the drift reversal capability and its external controllability are demonstrated for QAS and QPS stellarators, by which the impact of magnetic configuration on turbulent transport can be studied in experiments.

## 1. Introduction

Improved plasma confinement has been realized in toroidal plasmas by the turbulent fluctuation suppression. This has been considered to be consistent with theoretical predictions for the stabilization of micro-instabilities [1]. Several kinds of micro-instabilities appear when the directions of the diamagnetic drift and the $\nabla B$ drift ($B$ is the magnetic field strength) are the same for trapped particles. The direction of $\nabla B$ drift precession can be expressed in terms of the radial derivative of the second adiabatic invariant $J$. The stability condition for them is derived as $\nabla P \bullet \nabla J > 0$ ($\nabla J<0$ for $\nabla P<0$) in terms of J and scalar plasma pressure $P$, which is called the maximum-$J$ criterion (drift reversal). This condition is realized by $q$ (safety factor) profile control (such as in reversed shear tokamaks) [1], control of the plasma cross-section (such as ellipticity) [2], plasma diamagnetism [3], and strong inhomogeneity of the radial electric field [4]. The experimental demonstration of a significant increase of confinement time in a spherator [5] when trapped particles are localized in a good curvature region is also considered as a remarkable example of this effect.

Innovative helical systems have been widely studied [6-10] based on the quasi-symmetry concept. It is worthwhile to examine the drift reversal capability in such configurations for significant guidance in the configuration design for possible turbulent suppression. Here, we note that the importance of a drift reversal capability for the design of helical systems was already pointed about one decade ago [11]. Its qualitative evaluations are now available as described in this paper.

## 2. Description of J-calculation

The second adiabatic invariant $J$ for trapped particles is defined as $J \equiv \int v_{||} dl$, where $dl$ denotes the line element along a magnetic field line and the integral is performed over a bounce period. For analytical simplicity, $J^* \equiv \int v_{||} d\zeta$, ($\zeta$ being the toroidal angle) has been frequently utilized, which is based on the assumption that the rotational transform per toroidal field period is sufficiently small that the integral path can be taken in the toroidal direction.

However, in this study, a direct calculation of $J$ is performed by following the guiding center of low energy trapped particles for which the deviation from a magnetic field line is negligibly small. The guiding center equations [12] are expressed by use of the Boozer coordinates ($\psi$, $\theta$, $\zeta$) [13], with $\psi$ being the normalized toroidal flux, and $\theta$ ($\zeta$) the poloidal (toroidal) angle. The motion of the guiding center is defined by five variables (($\psi$, $\theta$, $\zeta$) for the real space, velocity and the particle energy, $W$). Since the direction (sign) of the precession is the key for the stability condition, the $W$ dependence is not important here, so that particles with fixed $W$(=10eV) are considered. Also, the integral is performed along the particle trajectory so that one out of the $\theta$ and $\zeta$ dependences is omitted when the launching points of particles are specified. To obtain the radial profile of $J$, tracer particles which are to be reflected at the same $B$ are launched from the bottom of the dominant magnetic field ripple [e.g., the bottom of the toroidicity induced ripple ($\theta$=0) for QAS configurations, and that of the bumpy (poloidally symmetric) field-induced ripple ($\zeta/(2\pi/M)\equiv\zeta_N$=0.5) for QPS configurations]. Here, $M$ is the number of field periods. The initial velocity of tracer particles, $v_{\|,st}$, is defined as $v_{\|,st}=[2W(1-B_{st}/B_{ref})/m]^{1/2}$, where $B_{st}$ ($B_{ref}$) is the magnetic field strength at the initial (bounce) point and $m$ is the particle mass. It is noted that the specification of $B_{ref}$ corresponds to treating tracer particles with the same magnetic moment ($\mu$), which is an estimate of how deeply these particles are trapped in a magnetic ripple.

### 3.1. Drift reversal capability in QAS configurations

Configuration studies based on the QAS concept have been extensively developed in Japan (CHS-qa) [8] and in the USA (NCSX) [9]. In this section, the drift reversal capabilities in candidate configurations for both designs are described.

Firstly, the candidate configuration for CHS-qa (2w39) is examined. This particular configuration ($M$=2) has an aspect ratio of about 4.3, and the rotational transform lies between 0.37 and 0.4 with a slight increase towards the edge. Several non-axisymmetric components of B appear near the edge with a few percent of the uniform magnetic field strength.

Figure 1 shows contours of $J$ with $B_{ref}$=1.0 in the ($r/a$, $\zeta_N$) plane, with $r/a=\psi^{1/2}$, for a vacuum configuration. It shows the existence of a local maximum of $J$, which gives $dJ/dr<0$ (drift reversal) in the outer radii (hatched region). The local maximum of $J$ is created by the residual non-axisymmetry of $B$ in the edge region due to the larger reduction of the parallel velocity through the conservation of $\mu$ [14]. This feature is significantly unique for QAS configurations, and is not realized in axisymmetric tokamaks. The non-axisymmetry of $B$ can be externally controlled through configuration control, such as by shifting the magnetic axis inward/outward. In addition, large positive shear of the rotational transform (negative shear of $q$) can be realized with the sustenance of the rotational transform through the bootstrap current (in a region of large pressure gradient) and reduction of the central rotational

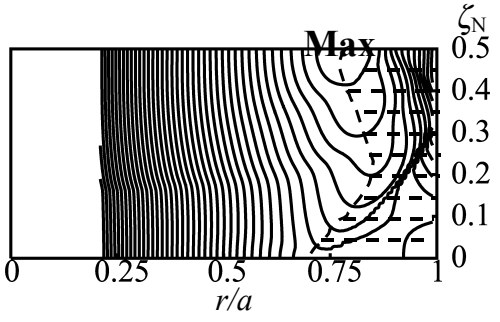


*FIG .1. Contours of J ($B_{ref}$=1.0) on (r/a, $\zeta_N$) plane for the candidate configuration of CHS-qa (2w39). The "Max" denotes the local maximum of J and the hatched region indicates the region where drift reversal is realized.*

transform by the Shafranov shift [15]. In such a case, tokamak-like drift reversal (due to the magnetic shear) is also possible in the core region, combined with the non-axisymmetry induced drift reversal in the edge region.

Secondly, a previous candidate configuration for NCSX (li383) is examined. This configuration has been obtained by a numerical optimization study, with a target $\beta$ value of about 4.1 % with $M$=3 (with a plasma current of about 125 kA for B=1.2T and a major radius of 1.4 m). Thus, the drift reversal capability is examined at this particular $\beta$ value. The rotational transform profile is shown in Fig. 2, where relatively large positive shear of the rotational transform (negative shear of $q$) exists, except very near the edge region. It also has a large radial variation of the uniform magnetic field component (corresponding to a deep magnetic well), which weakens the contribution of the non-axisymmetry of $B$ to the particle trajectories.

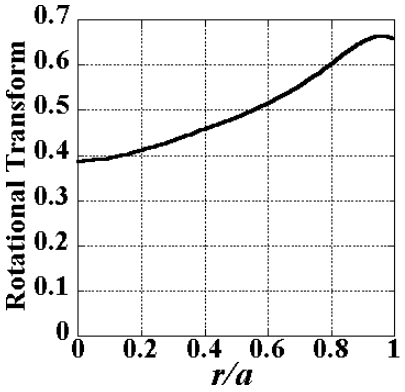


*FIG .2. The rotational transform for the li383 configuration at β=4.1%.*

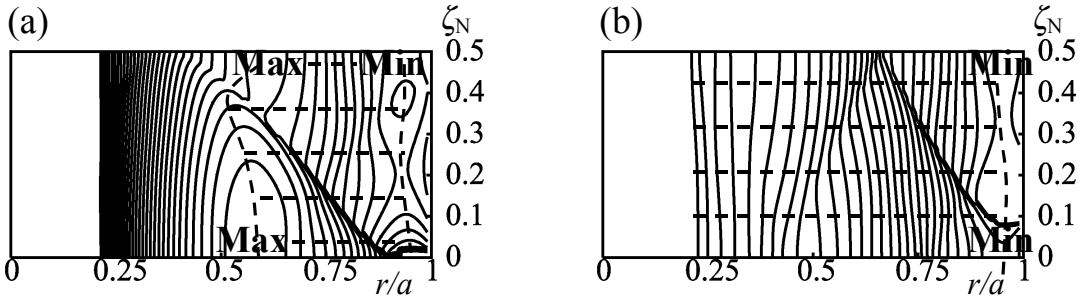


*FIG .3. Contours of J ((a) $B_{ref}$=0.98 and (b) $B_{ref}$=1.02) in the (r/a, $\zeta_N$) plane for the li383 configuration with β=4.1%. The "Max (Min)" denotes the local maximum (minimum) of J and the hatched region indicates the region where drift reversal is realized.*

Figure 3 shows contours of $J$ with (a) $B_{ref}$=0.98 and (b) $B_{ref}$=1.02 in the ($r/a$, $\zeta_N$) plane. For more deeply trapped particles (such as for the $B_{ref}$=0.98 case), the magnetic shear is not enough to realize drift reversal for the inner region. However, as $B_{ref}$ is increased (that is, as the degree of trapping becomes shallower), the region where drift reversal is possible extends towards the core region. It is recognized from Fig. 4 that the negative shear of the rotational transform (positive shear of $q$) in the very edge region avoids realizing drift reversal. In this sense, it can be remarked that the drift reversal capability of this configuration strongly depends on the magnetic shear, which is the same mechanism as that in reversed shear tokamaks.

The effects of non-axisymmetry of $B$, magnetic shear (mainly induced by the plasma current) on the drift reversal capability in CHS-qa and NCSX have been described in this section. They provide the "external knob" for the drift reversal capability in QAS configurations.

### 3.2. Drift reversal capability in a QPS configuration

As for the QPS category, an example configuration ($M$=4) [16] is investigated. The geometrical aspect ratio is about 10. This configuration has been obtained through plasma boundary shaping. There is a significant variation of area of magnetic surfaces in the toroidal direction. This gives the dominant bumpy component of $B$ through the conservation of toroidal magnetic flux. The bumpy field strength is as much as half of the uniform magnetic field strength. There still remain the symmetry breaking components such as those corresponding to the helicity and toroidicity. However, the amplitudes of these components are less than 1/5 of that of bumpy component, and also it should be noted that the toroidicity is reduced to a level about half of the geometrical inverse aspect ratio.

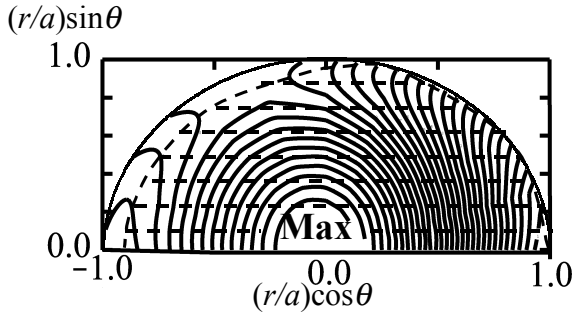


*FIG. 4. Contours of J ($B_{ref}$=0.65) in the (r/a, θ) plane for a QPS finite beta configuration. The "Max" denotes the maximum of J and the hatched region indicates the region where the drift reversal is realized.*

Figure 4 shows contours of $J$ (for $B_{ref}$=0.65, deeply trapped particles) in the ($r/a$, $\theta$) plane for a finite beta equilibrium (volume averaged $\beta$ value of about 5 %). $J$ is a maximum at the plasma core and radially decreases, which satisfies the condition $\nabla J<0$. It shows clear drift reversal. It is noted that drift reversal is not realized at vacuum for this particular configuration. It has a large bumpy field component with little radial variation of amplitude. At vacuum case, particles launched from $\zeta_N$=0.5 with constant $\mu$ perform similar bounce motion, which gives little radial variation of $J$ profile, since the bumpy field component has little radial variation (cf., Ref. [16]). This is still true even for a finite beta equilibrium. The vacuum magnetic well is much smaller compared to the amplitude of the dominant bumpy component. However, the magnetic well is enhanced up to about half of the bumpy component for the mentioned finite beta equilibrium, which establishes an absolute minimum of $B$ for the core region in the plane where particles are launched. This radial increase of $B$ towards the plasma edge plays an essential role for realizing a radially decreasing $J$ profile (drift reversal) as shown in Fig. 4. This is the unique mechanism for drift reversal in QPS configurations, which is different from that in QAS configurations. This would also be relevant for QPS configurations in the design phase at Oak Ridge National Laboratory [10], which are to be examined from the viewpoint of the drift reversal capability.

## 4. Conclusions

In conclusion, the drift reversal capability has been analyzed in innovative helical systems to investigate a possible approach towards improved confinement through turbulent transport suppression. The unique external knobs for drift reversal, the residual non-axisymmetry of $B$ for QAS and the magnetic well for QPS, are clarified in addition to the well-known magnetic shear contribution in axisymmetric tokamaks. The external controllability of the drift reversal capability is important in performing a systematic study of the impact of magnetic configuration on turbulent transport. These knobs provide additional approaches towards improved confinement in addition to those (e.g., heating power beyond some threshold value) utilized in previous experiments.

The favorable effect of drift reversal is anticipated to reduce the average bad curvature, so as to reduce the growth rate of instabilities such as trapped particle modes and temperature gradient modes. The relevance of the drift reversal capabilities is currently being examined through quantitative analysis of micro-instabilities by the FULL code [17]. So far, we have found the toroidal drift mode (trapped electron mode) in the collisionless electrostatic limit for the case shown in Fig. 1. The destabilization is dominated by the most deeply trapped particles for which drift reversal is the most difficult to realize due to the non-axisymmetry of $B$. More extensive and systematic estimate of microinstabilities in QAS and QPS configurations are to be performed to clarify the contribution of drift reversal in helical systems.

**Acknowledgements**

The authors gratefully acknowledge Dr. Long-Poe Ku (PPPL) for help with the equilibrium calculations required for the FULL code. This work has been supported by grants-in-aid for one of the authors (MY) from The Sumitomo Foundation and The Ministry of Education, Culture, Sports, Science, and Technology, Japan.

**References**

[1] KADOMTSEV, B.B., and POGUTSE, O.P., Reviews of Plasma Physics, Vol.5 (Consultants Bureau, New York, 1970), p.249.
[2] GLASSER, A.H., FRIEMAN, E.A., and YOSHIKAWA, S., Phys. Fluids **17** (1974) 181.
[3] ROSENBLUTH, M., and SLOAN, M.L., Phys. Fluids **14** (1971) 1725.
[4] ITOH, S.-I., and ITOH, K., J. Phys. Soc. Japan **59** (1990) 3815.
[5] YOSHIKAWA, S., Nucl. Fusion **13** (1973) 433.
[6] NÜHRENBERG, J., et al., Proc. Workshop on Theory of Fusion Plasmas (Varenna, 1994) (Bologna, Editrice Compositori) (1995) p.3.
[7] GARABEDIAN, P.R., Phys. Plasmas **3** (1996) 2483.
[8] OKAMURA, S., et al., Nucl. Fusion **41** (2001) 1865.
[9] NEILSON, G.H., et al., Phys. Plasmas **7** (2000) 1911.
[10] SPONG, D.A., et al., Nucl. Fusion **41** (2001) 711.
[11] ITOH, S.-I., Plasma Phys. Controlled Fusion **12** (1989) 133.
[12] FOWLER, R., er al., Phys. Fluids **28** (1985) 338.
[13] BOOZER, A.H., Phys. Fluids **23** (1980) 904.
[14] YOKOYAMA, M., et al., Phys. Rev. E **64** (2001) R15401.
[15] YOKOYAMA, M., et al., Nucl. Fusion **42** (2002) 1094.
[16] YOKOYAMA, M., et al., Nucl. Fusion **38** (1998) 68.
[17] REWOLDT, G., et al., Phys. Plasmas **6** (1999) 4705.